A PHOTOSYNTHESIS-BASED DRY DEPOSITION MODELING APPROACH

DEV DUTTA S. NIYOGI[1]*, KIRAN ALAPATY[2] and SETHU RAMAN[1]
[1] *Department of Marine, Earth, and Atmospheric Sciences, North Carolina State University, Raleigh, North Carolina, U.S.A.;* [2] *MCNC-Environmental Programs, Research Triangle Park, North Carolina, U.S.A.*
(author for correspondence, e-mail: dev_niyogi@ncsu.edu, Fax: +1 919 515 1441)*

(Received 9 February 2001; accepted 21 August 2002)

Abstract. We present a dry deposition modeling approach that includes vegetation-atmosphere interactions through photosynthesis/carbon assimilation relationships. Gas deposition velocity (V_d) is calculated using an electrical resistance-analog approach in a coupled soil-vegetation-atmosphere transfer (SVAT) model. For this, a photosynthesis-based surface evapotranspiration and gas exchange model is dynamically coupled to an atmospheric model with prognostic soil hydrology and surface energy balance. The effective surface resistance (composed of aerodynamic, boundary layer, and canopy-based resistances) is calculated for a realistic and fully interactive estimation of gaseous deposition velocity over natural surfaces. Based on this coupled framework, the photosynthesis-based gas deposition approach is evaluated using observed deposition velocity estimates for ozone over a soybean field (C3 photosynthesis pathway) and a corn field (C4 photosynthesis pathway). Overall, observed V_d and modeled V_d show good qualitative and quantitative agreement. Results suggest that photosynthesis-based physiological approaches can be adopted to efficiently develop deposition velocity estimates over natural surfaces. Such a physiological approach can also be used for generalizing results from field measurements and for investigating the controlling relationships among various atmospheric and surface variables in estimating deposition velocity.

Keywords: air pollution, biosphere-atmosphere interaction, dry deposition, photosynthesis, soil-vegetation-atmosphere transfer, terrestrial ecosystem

1. Introduction

Atmospheric deposition plays an active role in determining the air, water, and soil quality on a regional scale. A toxin deposited over land or water can, through the soil-vegetation-atmosphere continuum, affect regional hydrology and air quality at both diurnal and climatic scales (Niyogi and Raman, 2000). These interactions introduce variability and uncertainty in the regional ecosystem response to changes in the pollutant loading. Further, gaseous deposition is known to be actively responsible for various environmental problems associated with soil acidification, nutrient loading in watershed regions, and agricultural productivity at a regional scale (Hampp, 1992). Hence, understanding the deposition and fate of gaseous compounds over natural surfaces is an important component of environmental assessment programs.

Water, Air, and Soil Pollution **144:** 171–194, 2003.

The issue of pollutant deposition has been addressed mainly through measurements and integrated monitoring assessments (Fowler *et al.*, 1998; NCDENR, 1999). Measurements are often point based (as opposed to area based), however, and are only snapshot representations of the prevalent environmental conditions. Therefore, to complement the observations for spatially and temporally variable environmental conditions, a modeling approach is often required (Meyers *et al.*, 1998). Further, the nonlinear interactions between the atmosphere and surface vegetation make the deposition assessment over vegetated surfaces very uncertain (Cooter and Schwede, 2000). The development of realistic models can thus be useful for providing 'what if' scenarios for evolving and testing control and abatement plans. These can in turn assist an effective monitoring strategy by identifying potential concentration 'hot spots' and emission sources. Hence, it is important to have realistic, process-based gas deposition models (Wesely, 1989).

2. Objective

Analysis of dry deposition (the direct transfer of gases to surfaces) requires detailed representations of the surface-atmosphere exchanges and needs to be addressed as a continuum problem between the soil, vegetation, and the atmosphere (Baldocchi *et al.*, 1988; Wesely and Hicks, 2000). Field experiments (e.g. Garland, 1977) aver that canopy processes are a critical component affecting gas deposition over natural surfaces (Wesely and Hicks, 2000).

A number of deposition velocity models represent the vegetative processes in a relatively linear manner, as a meteorological feedback from the environment, following a Jarvis-type (Jarvis, 1976) approach (e.g., Baldocchi *et al.*, 1988; Hicks and Matt, 1988; Kramm *et al.*, 1996). As discussed in Cooter and Schwede (2000), the diagnostic canopy resistance estimates in the present-day (Jarvis-based) deposition models make the response prone to large uncertainties. The dependence of the deposition velocity estimates on the prescribed minimum stomatal resistance values is a serious issue (Niyogi and Raman, 1997). This is because, the minimum stomatal resistance term varies not only for vegetation types, but also has temporal (seasonal) variation. Further, it can only be estimated from field observations (as the lowest observed stomatal resistance under 'optimal' environmental conditions), and its estimation cannot be standardized through laboratory measurements, for instance. Additionally, the deposition models appear to perform better, particularly over vegetated surfaces, when detailed biophysical representation is included (Wesely and Hicks, 2000).

Recently, Niyogi and Raman (1997) and Niyogi *et al.* (1998) reviewed various advances in modeling the plant biophysical processes (cf. Farquhar *et al.*, 1980; Ball *et al.*, 1987; Noilhan and Planton, 1989; Collatz *et al.*, 1991, 1992; Sellers *et al.*, 1996). They concluded that the physiologically intensive schemes linking carbon assimilation and photosynthesis are superior in their ability to simulate the canopy resistances and surface-atmosphere exchanges for environmental applications. Additionally, studies such as Meyers *et al*. (1998), Niyogi and Raman (2000), and Finkelstein *et al*. (2000) conclude that detailed biophysical vegetation models are necessary for estimating gas deposition to natural surfaces. Thus, inductively it follows that the photosynthesis-based physiological schemes can be effectively applied for modeling gas deposition velocities over vegetated/natural surfaces (see also Wesely and Hicks, 2000). This hypothesis, however, has not been evaluated in an environmental model. Our objective is to test such a photosynthesis-based modeling approach for estimating dry deposition velocities in a terrestrial ecological perspective. This research objective is also consistent with the operational requirements posed by the environmental regulatory agencies in the United States (cf. Meyers *et al*., 1998; NCDENR, 1999; Valigura *et al*., 2000; NRC, 2000), particularly for deposition related to the primary pollutants (Niyogi *et al*., 1999a). We provide a validation of the photosynthesis-based model as a viable approach for assessing dry deposition velocity, in a coupled modeling framework. A follow up study underway, compares the hierarchy of biophysical representations for deposition velocity estimates over continental United States during summer of 1996 and will be reported shortly (Alapaty *et al*., 2002, manuscript in preparation).

Section 3 presents a generalized theory and formulations dealing with the deposition velocity (V_d) models, and outlines the photosynthesis-based, coupled soil-vegetation-atmosphere transfer (SVAT) modeling approach adopted in this study. Results are discussed in Section 4, and Section 5 gives a summary and conclusions.

3. Estimating Deposition Velocity

Deposition velocity (V_d) is a convenient way to parameterize pollutant deposition representative of the particular surface conditions and gas characteristics. The deposition flux, F_d, which is the amount of deposited material per unit surface area per unit time, is defined as the product of deposition velocity and mean gas concentration, C:

$$F_d = V_d C \ . \tag{1}$$

Equation (1) is useful for both modeling and field experiments. Generally, V_d values for different gases and surface characteristics are available in the literature (e.g., Walmsley and Wesely, 1996) and assumed to vary over a small range under similar conditions. By knowing ambient pollutant concentrations either through measurements (e.g., Padro, 1994) or by applying air quality models (e.g., Chang *et al*., 1987), and by prescribing deposition velocity from look-up tables or by using dynamic formulations (presented ahead), deposition flux can be estimated (e.g., Wesely, 1989).

Consistent with Equation (1), deposition velocity can be estimated using micrometeorological observations of F_d and C (Arya, 1988). However, even measurements have inherent limitations, generally in terms of the limited range of data and variability in the atmospheric conditions, as well as from heterogeneity in the sensor footprint (Erisman *et al*., 1994). Hence there is an ongoing need for parameterizations that can accurately estimate deposition velocity both for observed concentrations and for numerical/diagnostic models (Wesely, 1989).

In parameterizing deposition velocity, often a resistance pathway is adopted (e.g., Garland, 1977). The larger the material's resistance to deposit, the lesser is the deposition flux. Further, following Equation (1), deposition flux is directly proportional to V_d. One thus obtains deposition velocity as the inverse of total resistance (Baldocchi *et al*., 1988). The depositing surface offers resistance through different pathways: soil surface, leaf cuticles, stomata and mesophyll, and the aerodynamics of the surface and the boundary layer around the surface, as described in Wesely (1989). Generally, the resistance pathways can be categorized as aerodynamic resistance (R_a), surface quasi-laminar boundary resistance (R_b), and canopy-based resistance (R_c), giving,

$$V_d = (R_a + R_b + R_c)^{-1} . \quad (2)$$

A schematic representation of such a resistance pathway for surface deposition is shown in Figure 1. Of these three resistances, the R_c term is dominant for dry deposition (Baldocchi *et al*., 1988). In this study, we estimate R_a and R_b using parameterizations based on vegetation-atmosphere interactions, and obtain R_c with a photosynthesis-based approach. All the resistances are dynamically interactive and modulate the deposition potential to the surface, and are estimated by linking a detailed, physiologically intensive vegetation and gas exchange scheme called Gas Exchange/photosynthesis based Evapotranspiration Model: GEM (Niyogi, 2000; Niyogi *et al*., 1999a–c, 2000) with a prognostic atmospheric boundary layer model (Alapaty *et al*., 1997). The formulations describing the submodels are discussed in the appendix; a brief summary is presented here.

Soil-vegetation-atmosphere transfer (SVAT) is an inherent feature of gas exchange and deposition processes. Considering the parameters in Equation (2), the aerodynamic resistance can be parameterized as (e.g., Baldocchi *et al*., 1988).

$$R_a = Pr(\ln z/z_o - \psi_h)(ku_*)^{-1} , \quad (3)$$

where Pr is the Prandtl number, often considered equal to 0.923 (Draxler and Hess, 1997); z is measurement height (m), and z_o is the roughness length (m); k is the von Karman constant (equal to 0.4); ψ_h is a similarity-based nondimensional stability correction term (Businger *et al*., 1971); and u_* is the surface friction velocity (ms^{-1}). In our coupled modeling framework, these variables are obtained from the surface layer similarity relationships (Arya, 1988) used in the Alapaty *et al.* (1997) atmospheric boundary layer model. The roughness length can be prescribed as a function of land use following Wieringa (1993) and Davenport *et al*. (2000). Alternatively, if the vegetation canopy height, h_c, and the leaf area index, *LAI*, are

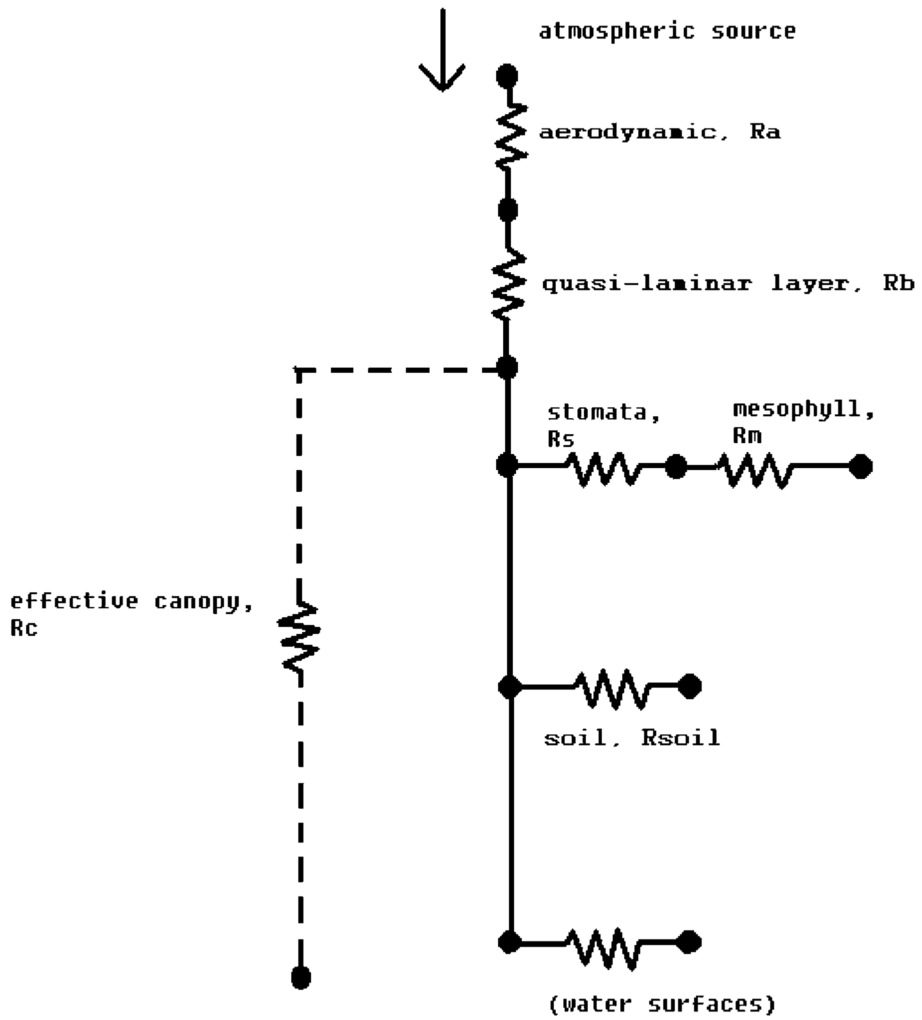

Figure 1. Surface resistance pathways for the deposition gases. Inverse of the total resistance offered by R_a, R_b, and R_c yields deposition velocity (V_d) (After Baldocchi *et al.*, 1988; Weseley and Hicks, 2000).

known, z_o can be calculated following Shaw and Perriera (1982) and Meyers *et al.* (1998):

$$z_o = h_c \cdot \left(0.215 - \frac{LAI^{0.25}}{10}\right) . \tag{4}$$

For estimating the quasi-laminar sublayer/boundary layer resistance (R_b), we adopt an approach developed by Nikolov *et al.* (1995) and Su *et al.* (1996), and described in Niyogi *et al.* (2000). In this, the boundary layer resistance is calculated for two conditions: forced convection (R_{bfc}) and free convection (R_{bfr}). Accordingly,

$$\frac{1}{R_{bfc}} = cT^{0.56}\left[(T + 120)\,\frac{u}{dP}\right]^{0.5} , \tag{5}$$

where c is the transfer coefficient (equal to 4.322×10^{-3} for broad leaves and 1.2035×10^{-3} for conifers, following Nikolov *et al.* (1995)), T is the ambient air temperature (K), u is the wind speed (ms^{-1}), d is leaf length scale (m), and P is the ambient pressure (Pa). For a free convection boundary layer, the equation is of the form

$$\frac{1}{R_{bfr}} = cT_s^{0.56}\left\{\frac{T_s + 120.0}{P}\right\}^{0.5}\left\{\frac{T_{vs} - T_{va}}{d}\right\}^{0.25} , \tag{6}$$

in which T_s is the surface temperature (K); T_{vs} and T_{va} are the virtual surface and air temperatures, respectively (Arya, 1988). R_b is taken as the smaller of the two resistances R_{bfc} and R_{bfr}.

Knowing R_a (Equation (3)) and R_b, estimates of R_c are needed to parameterize the surface resistance term for estimating deposition velocity. Typically, the R_c term has been represented as a combination of various resistances at the surface through the vegetation and the atmosphere (via leaf-scale gas-assimilation photosynthesis, evapotranspiration, and energy balance), for mass and energy transfer as well as gas exchange (Niyogi and Raman, 1997, 2000; Wesely and Hicks, 2000). Note that for environmental problems, it is critical to parameterize the stomatal pathways correctly. This is due not only to the dominance of the R_c term in calculating daytime V_d, but also to the involvement of the stomatal (and cuticular) pathways in generating the source/sink conditions for biogenic volatile organic compounds when ‘compensation point’ conditions are additionally considered (Rondon and Granat, 1994; Sutton *et al.*, 1998; Niyogi and Raman, 2000; Nemitz *et al.*, 2000).

The canopy-based resistance is taken as the inverse of leaf conductance, which is scaled to the canopy conductance through the leaf area index. The leaf conductance is semi-empirically linked to the photosynthesis (carbon assimilation) rate following Ball *et al.* (1987). Carbon assimilation is the residue of the gross assimilation and loss due to respiration. Gross assimilation is calculated as a function of plant characteristics, photosynthesis pathway, soil moisture, ambient temperature, and land use following Collatz *et al.* (1991, 1992) and Sellers *et al.* (1996). The respiration loss is parameterized using information on maximum assimilation rate and mesophyllic conductance of the vegetation, following Calvet *et al.* (1998). Following Wesely (1989), the gas exchange is modeled for carbon dioxide and then, using the ratios of the diffusivities between the depositing gas and CO_2, the results are extended for exchange and deposition characteristics for different gases.

The canopy resistance for water vapor estimated in the photosynthesis module is linked with a prognostic soil moisture and soil temperature model following Noilhan and Planton (1989) and Alapaty *et al.* (1997). In the soil model, four prognostic equations for topsoil (0.1 m deep) and deep soil (1 m) temperature and moisture are solved, plus one for rainfall interception. This hydrological module provides surface boundary condition for a one-dimensional (1-D) atmospheric model as described in Alapaty *et al.* (1997). In our study, we use this 1-D model, which has 35 vertical layers, follows surface layer similarity relationships (Arya, 1988), and uses a mixed-layer parameterization that is based on turbulent kinetic energy (Mellor and Yamada, 1974). Though the model is integrated in 1-D form, it has the capability to ingest prescribed large-scale wind and thermodynamic fields either from observations or from a 3-D model analysis. The appendix presents more details on the atmospheric and soil models as well as on the photosynthesis-based model and its coupling to the atmospheric model through the surface energy balance approach. The process flow between the different modules and their coupling is summarized in Figure 2.

4. Model Simulations

In this section, the feasibility of the photosynthesis-based deposition velocity modeling approach is tested. We perform and discuss the results of validation case studies using actual field observations for ozone deposition velocity, over agricultural landscapes.

The validation data we used are from a field campaign conducted for measuring ozone deposition velocity over various natural surfaces. Details regarding the observational setup, instrumentation, and the field campaign can be found in Meyers *et al.* (1998). For validating our scheme, we used the observations made over a soybean field near Nashville, Tennessee, and over a corn field near Bondville, Illinois; these two sites were selected because soybean represents a C3 photosynthesis pathway while corn follows a C4 pathway. The model needed to be tested for both the photosynthesis pathways because: (i) physiological studies indicate different biophysical responses for similar environmental stress for C3 and C4 vegetation; and (ii) there are separate parameterizations in the model depending on whether the vegetation shows C3 or C4 pathway (e.g. Farquhar *et al.*, 1980; Collatz *et al.*, 1992). Meyers *et al.* (1998) obtained observed ozone V_d values as a ratio of ozone flux direct measurements and ambient ozone concentration measurements. Ozone concentrations were continuously monitored using a UV photometric ambient ozone analyzer, and only values above 5 ppb were considered reliable for developing the V_d estimates (Meyers *et al.*, 1998, for instrumentation details). Ozone fluxes were estimated using the eddy covariance approach. Fast response ($\sim$5 Hz) ozone measurements were made using a chemiluminescent analyzer, while the vertical velocities were measured using a three-axis sonic an-

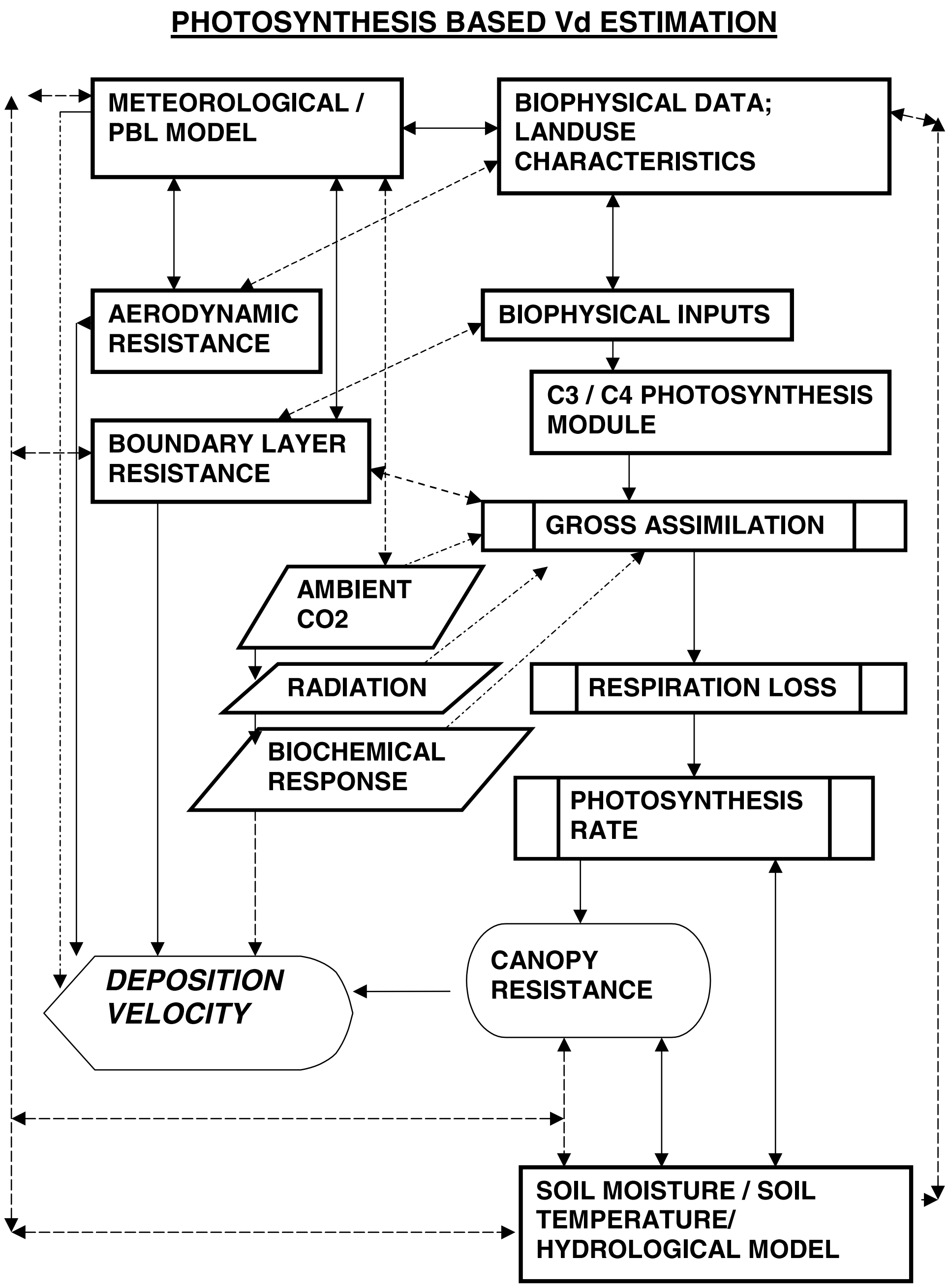

Figure 2. Process flowchart of the photosynthesis based deposition velocity estimation approach adopted in this study. The atmospheric boundary layer model, is coupled to a prognostic soil moisture/soil temperature, and to a photosynthesis-based vegetation scheme. Solid lines indicate variables are passed from one module to the other directly; dashed lines indicate interactive coupling or dependency of the two modules through coupled parameterizations.

emometer. Meyers *et al*. (1998) indicate an uncertainty level of about 15–20% in the ozone V_d estimates.

We performed one set of model simulations over a soybean field (C3 pathway) located at 36.65°N, 87.03°W, near Nashville, Tennessee, for two different periods: 6–8 August, 1995 and 12–14 September, 1995. These two periods were in contrast, in terms of both the vegetation characteristics and the soil moisture conditions. The August case represents relatively higher soil moisture availability and denser vegetation (LAI around 6.0). The September case shows nearly drought-like conditions, with a reduced canopy density (LAI around 3.0) along with some drying of the leaves. The second set of validation simulations was performed over a corn field (C4 pathway) located at 40.05°N, 88.37°W, near Bondville, Illinois. For this site also, two regimes were selected: a fully vegetated but relatively dry period on 24–25 August, 1994, and a relatively wet and lesser-vegetated period on 15–16 September, 1994.

For both the sites, surface meteorological observations as well as biophysical conditions were obtained following Meyers *et al*. (1998) and Finkelstein (2000, personal communication from P. Finkelstein of NOAA/ERL/ARL). In addition to the observations at the surface, the atmospheric model requires information on the winds and thermodynamic state along the model column (about 5 km deep). Since 'upper-air' observations were not available as part of the field campaigns, this information was obtained from an archived U.S. National Center for Environmental Prediction (NCEP) Nested Grid Model/Regional Analysis and Forecast System (NGM/RAFS) northern hemisphere analysis (Hoke *et al*., 1989) over the study site. The ABL model (Alapaty *et al*., 1997) coupled to the GEM-based physiological V_d estimation scheme was initialized with a representative sounding at 0600 LT (obtained from the NGM/RAFS-analyzed fields) over both study regions, and the model was integrated for 48 hr.

4.1. Validation over C3 vegetation in Nashville

Figure 3 shows the model-simulated and corresponding observed ozone V_d values for the Nashville case. On 6 August, observations show V_d values that typically range around 1×10^{-2} ms^{-1} during the day and start decreasing in the evening around 1600 LT. This occurs because the daytime canopy resistance values typically are small and then increase in the evening, leading to lower deposition velocities. The GEM-simulated deposition estimates, though relatively higher, follow a similar trend. Consistent with the observations, the model simulates high V_d values (1.5×10^{-2} ms^{-1}) around noon ($\sim$1100 LT); then, in the later part of the evening (after 1800 LT), the values reduce significantly (around 0.1×10^{-2} ms^{-1}) as the vegetation processes become inactive. Overall, despite the daytime over prediction, considering the uncertainty in prescribing the initial conditions, the modeled and the observed V_d values for 6 August are in fair agreement. The daytime over prediction for 6 August does not appear to be a consistent model bias, since for 7 August, the model underpredicts the early morning V_d values, and responds well to the environmental changes. The daytime deposition velocities are around 1.5×10^{-2} ms^{-1}, which are generally consistent with the observations. Thus, the dynamical model appears to have captured both the day-to-day and the short-term/hourly variations in the observed deposition velocity estimates. Two features stand out in this case study. First, the physiological scheme successfully reproduced the day-to-day variation in V_d, with relatively constant daytime values on 6 August and more variable V_d values on 7 August. Second, the model estimates are in fair agreement with the observations.

Figure 4 shows the model results and corresponding observations for ozone deposition velocity for the 12–13 September case. Compared to the August case, the September period was relatively drier and the vegetation showed signs of wilting stress. Such surface conditions lead to high canopy resistances, which generally lead to lower V_d values. This is reflected in the V_d observations; for this case, the V_d values were around 0.5×10^{-2} ms^{-1} (Meyers *et al.*, 1998), which is nearly 50% less than the average observed values in the august case. The model captured these changes quite well. For the 12 September case shown in Figure 4a, the modeled V_d values in the early morning and late evening period are around 0.4×10^{-2} ms^{-1}, and increase to around 0.6×10^{-2} ms^{-1} during the afternoon. As also concluded by Meyers *et al.* (1998), this case does not show significant diurnal changes like those seen for the wetter and more densely vegetated August case. This is because the vegetation does not actively respond to the environmental changes when it is wilting (Avissar *et al.*, 1985). For both 12 and 13 September (Figure 4b), the model captures the damped diurnal V_d variations quite satisfactorily. This is especially notable because the September field conditions in this case, are relatively difficult to simulate due to the wilted patches in the vegetation. As discussed in Makela *et al.* (1996), Niyogi and Raman (1997), and Giorio *et al.*, (1999), the interactions between soil moisture deficit and photosynthesis are in general poorly represented in the photosynthesis-based schemes; the results from the September case tend to support this.

Further, for 6 and 7 August the model underpredicts V_d in the morning and overpredicts it in the evening. In other words, the modeled resistances are higher than those observed in the mornings, and lower than the observed values in the evenings. One possible explanation is that, in the field observations, the vegetation could be showing an enhanced response to red light compared with its response to other components of solar radiation, as recently reported in Musselman and Minnick (2000). This response to a specific radiative component (as opposed to the total radiation on vegetation) is not included in the photosynthesis-based model, presently. These hydrological and radiative interactions in the photosynthesis-based models should be addressed in future studies. For the afternoon conditions, the model response shows a positive bias for one day and a negative bias for the other. Since the model performance is relatively poor for the September case, we examined the temporal bias plots (not shown). Overall, there is no consistent model bias, and the

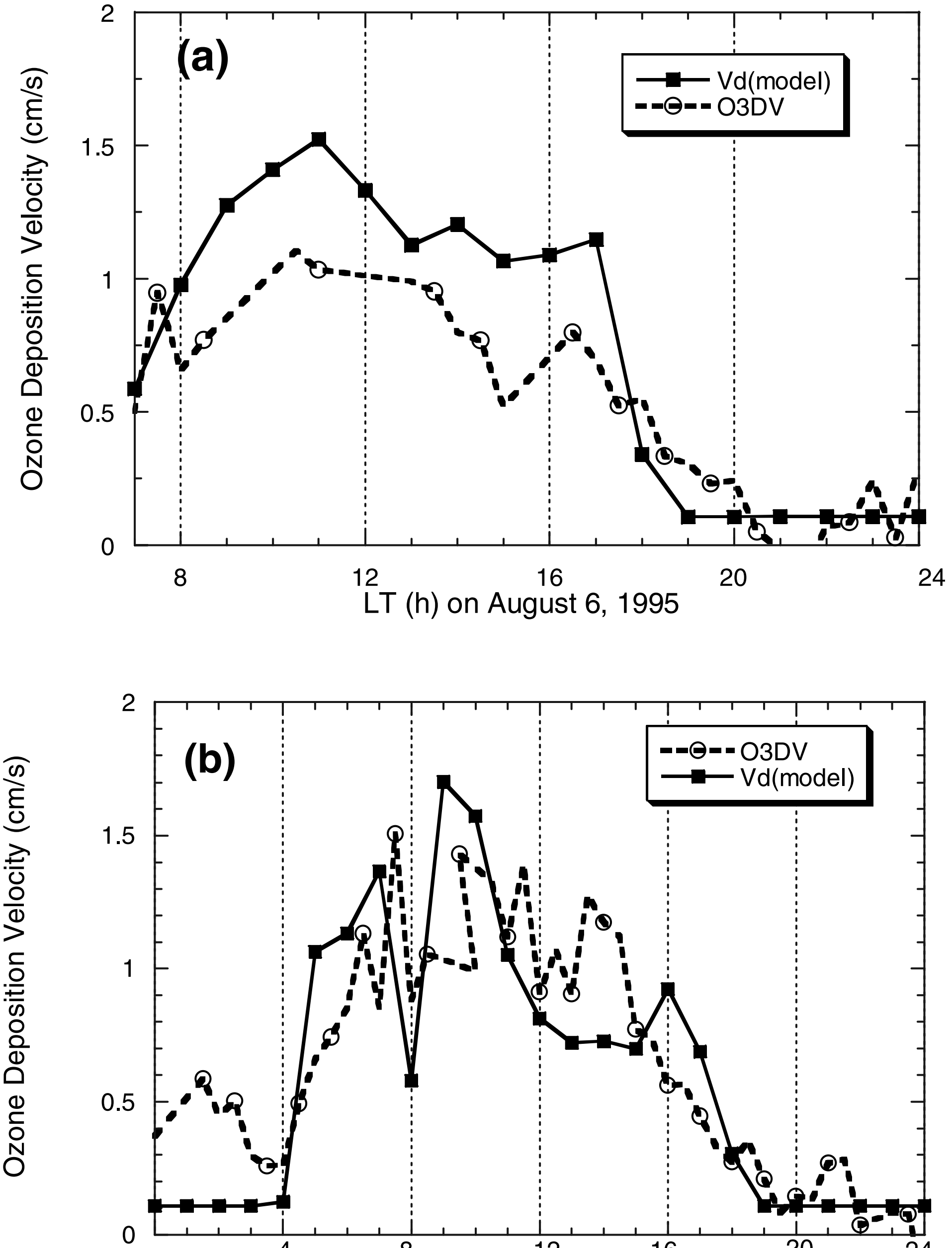

Figure 3. Observed ('O3DV') and modeled ozone deposition velocity (cm s^{-1}) over a soybean field near Nashville, TN, for (a) 6 August, 1995, and (b) 7 August, 1995. The vegetation was fully grown with high soil moisture availability.

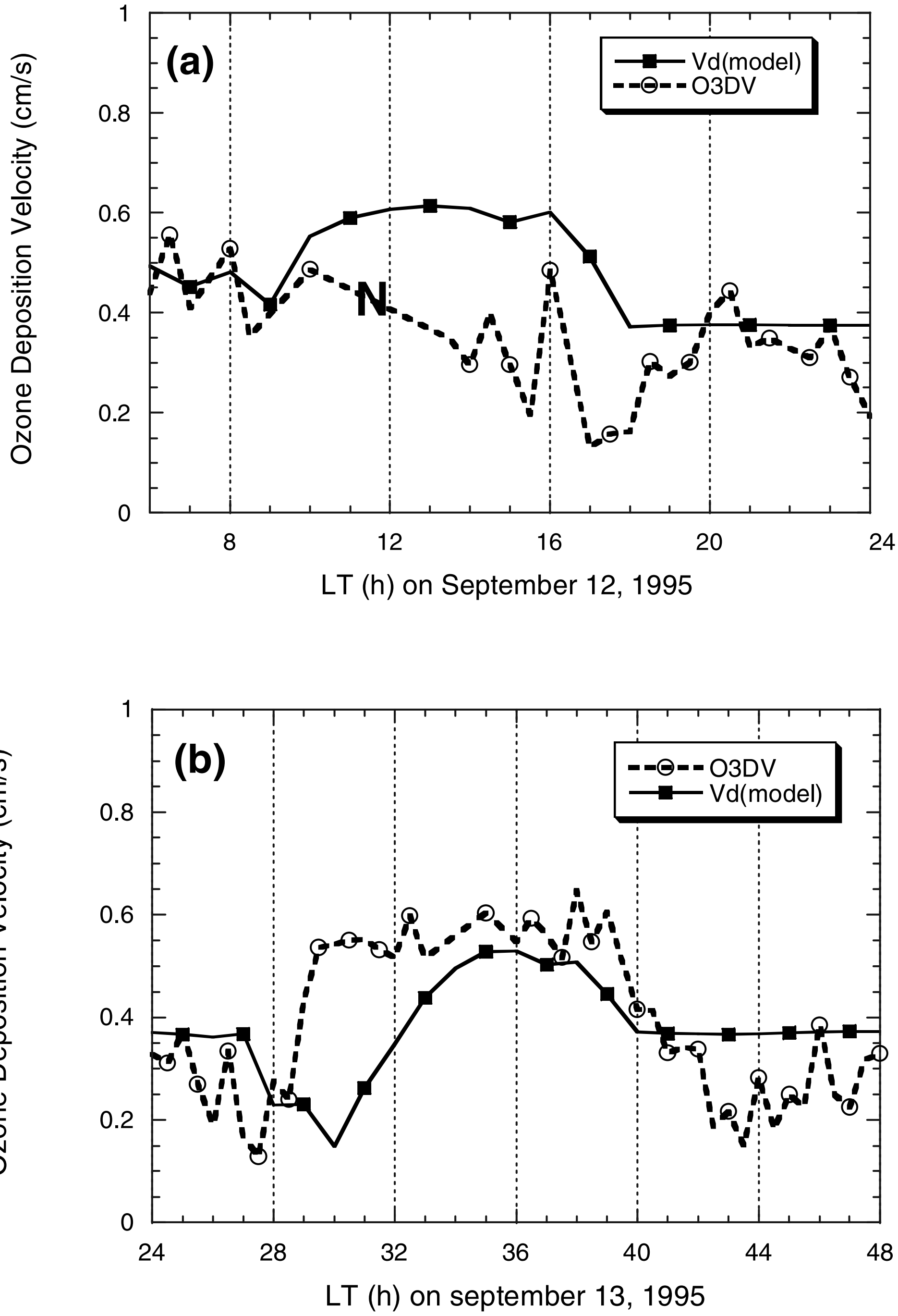

Figure 4. Observed ('O3DV') and modeled ozone deposition velocity (cm s^{-1}) over a soybean field near Nashville, TN, for (a) 12 September, 1995, and (b) 13 September, 1995. The vegetation was drying and soil moisture availability was low. For the observations, 'N' means 'No Data'.

quantitative difference between modeled and observed V_d is small for the two days. In general, the coupled deposition model performance over the C3 canopy was satisfactory in its ability to simulate deposition velocity estimates under different environmental conditions.

4.2. Validation over C4 vegetation in Bondville

Figure 5 shows the observed and modeled time series for 24 and 25 August, 1994. For this period, the vegetation (corn) is fully grown, and the soil moisture availability is moderate to low. Typical observed daytime ozone V_d values are around 0.6×10^{-2} ms^{-1}, with maxima of 0.7×10^{-2} ms^{-1} and 0.8×10^{-2} ms^{-1} for the two days. In general, the model-estimated deposition velocities are slightly lower than the observations but there is good qualitative and quantitative agreement. On 24 August (Figure 5a), the simulations follow the observations quite closely for the early morning and later part of the evening, while for the afternoon conditions there is significant underprediction. However, the afternoon peak in the V_d values and the associated variability is well captured, and the trend in the deposition velocity variations is also well simulated. Similar model performance is seen for 25 August (Figure 5b). The model underpredicts V_d values for the early morning, but the model quickly adjusts to the changes in the environment, providing good estimates of the deposition velocities for the rest of the day. The model captures a small peak, followed by a drop in the V_d values around 0800 to 0900 LT, then a steady rise in the deposition velocities until about noon. The peak simulated V_d value is around 0.7×10^{-2} ms^{-1} as compared to the observed peak V_d value of around 0.8×10^{-2} ms^{-1}. Again, as in the Nashville simulations, the photosynthesis-based model satisfactorily estimated deposition velocities consistent with the observations.

The overall underprediction in the deposition velocities in the Bondville case could be due to simulated canopy resistance values that are higher than the actual values over the corn field. The overestimated R_c values may be attributable to the complexity inherent in modeling vegetation exchanges under low soil moisture availability conditions (cf. Meyers *et al.*, 1998; Calvet *et al.*, 1999; Giorio *et al.*, 1999).

The second period considered for this case was 15–16 September, 1994. During this period the corn crop was relatively dry with smaller LAI (by about half), but the soil moisture availability is significantly higher than in the August case. Figure 6 shows the modeled and observed deposition velocity time series for the two days. For the September case, the observed daytime deposition velocities are around 0.25×10^{-2} ms^{-1}, while for the August case the daytime V_d values were around 0.6×10^{-2} ms^{-1}; this difference is indicative of the reduced vegetation canopy resistance of the drier September crop. The model estimates are similar to the observations. For 15 September, the observations show a peak deposition velocity around 0.3×10^{-2} ms^{-1} at approximately 0600 LT in the morning, fol-

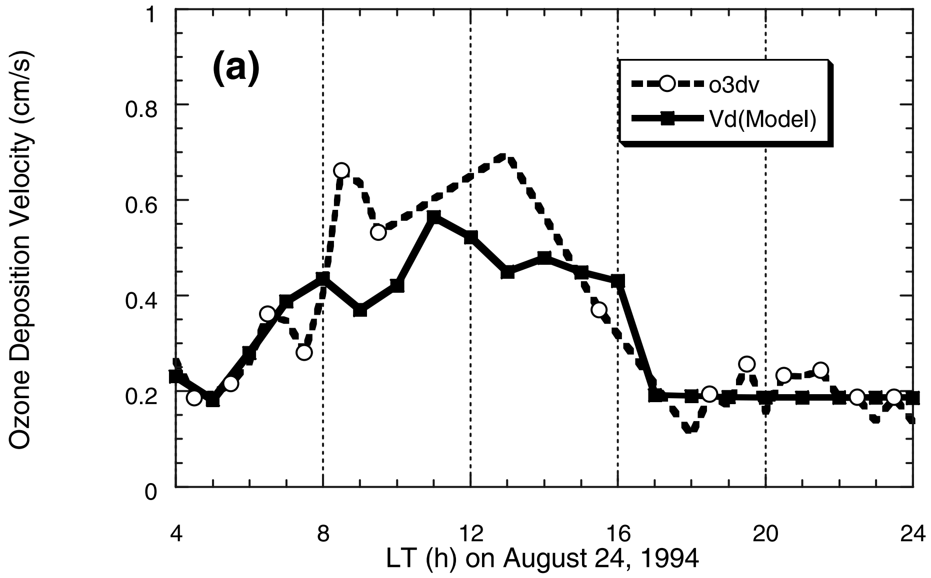

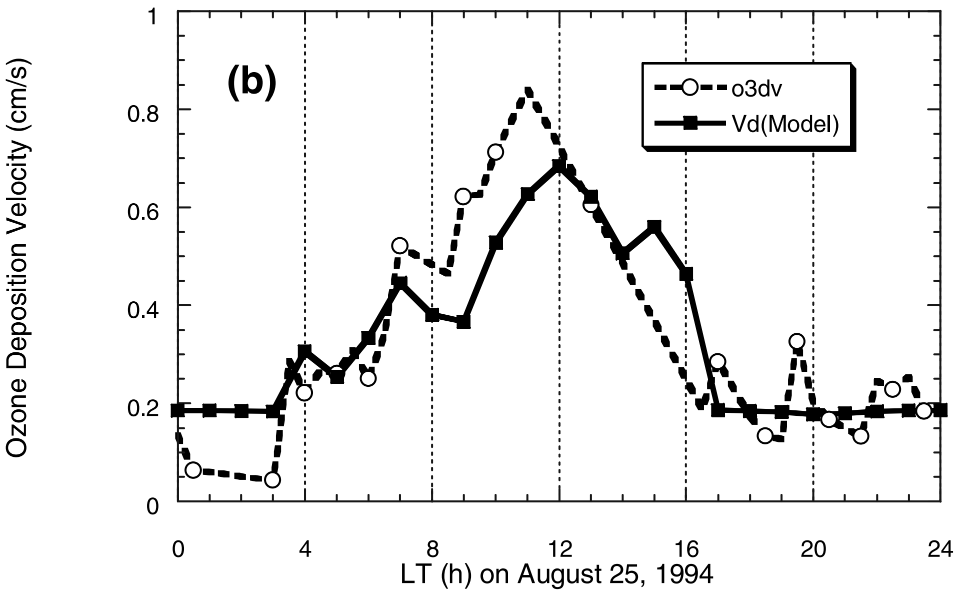

Figure 5. Observed ('o3dv') and modeled ozone deposition velocity (cm s^{-1}) over a corn field near Bondville, IL, for (a) 24 August, 1994, and (b) 25 August, 1994. The vegetation was fully grown and soil moisture availability was low to moderate.

lowed by a drop to about half the peak value. This spike in the morning deposition velocity could be due to changes in the atmospheric stability or some other site specific micrometeorological, fetch related issue that could be investigated further from the observations. Over the day, the observed ozone deposition velocities vary between 0.2×10^{-2} ms^{-1} and 0.3×10^{-2} ms^{-1}. The modeled values generally follow the observations quite well. In the early morning, the modeled V_d values show a slight increase and then fall around 0600 LT to approximately 0.17×10^{-2} ms^{-1}. However, the model then tends to steadily overestimate until noon, with V_d values around 0.25×10^{-2} ms^{-1}. Around 1700 LT, the deposition velocities fall to around 0.07×10^{-2} ms^{-1}.

For the following day, 16 September, observations are available only until noon. The V_d observations show relatively small values around 0.07×10^{-2} ms^{-1} in the early part of the morning, with a small peak around 0.17×10^{-2} ms^{-1} at 0600 LT. During the day, V_d values reach a maximum of around 0.35×10^{-2} ms^{-1}. The model results generally follow the observations well. Until sunrise at 0530 LT, the modeled V_d is around 0.05×10^{-2} ms^{-1}; it then rises to 0.17×10^{-2} ms^{-1} in the early part of the day, peaking at a midday value of about 0.3×10^{-2} ms^{-1}. At 1700 LT the modeled V_d values are small again, around 0.05×10^{-2} ms^{-1}.

For both cases over C4 vegetation, there is fair agreement between the observations and the simulated velocities. Results also indicate that the model may be underpredicting the C4 crop deposition values, but the temporal variations are generally consistent with observations (and within 0.25×10^{-2} ms^{-1}). For the August case, which has lower soil moisture availability, the model generally underpredicts the deposition velocities in the afternoon, and shows the highest bias in the afternoon period. For the September case, with higher soil moisture availability, the biggest differences appear in the early morning and late evening periods, when the model tends to make the canopy effects inactive. These results again suggest that the bias could be due to an interactive effect of uncertainties in the model physics as well as to the prescribed values of LAI and soil moisture (Niyogi *et al.*, 1999d).

4.3. Summary of Case Study Results

In summary, an interesting feature of these case studies is that the photosynthesis-based model was able to capture both the seasonal and the diurnal changes fairly well, for both the C3 and C4 cases. This performance was achieved without any ‘tuning’ of the vegetation parameters (which is often required for the non-photosynthesis-based models, as discussed in Cooter and Schwede (2000)). From the model comparison, some of the individual modeled V_d values were significantly different (by about 30%) than the corresponding observations. These differences could be due to a number of interactive factors, which include inherent model and observational uncertainties (Niyogi *et al.*, 1999d); the differences between the observed meteorology and the dynamic-model-generated meteorology; and the uncertainty in specifying the surface hydrometeorological conditions (Alapaty *et*

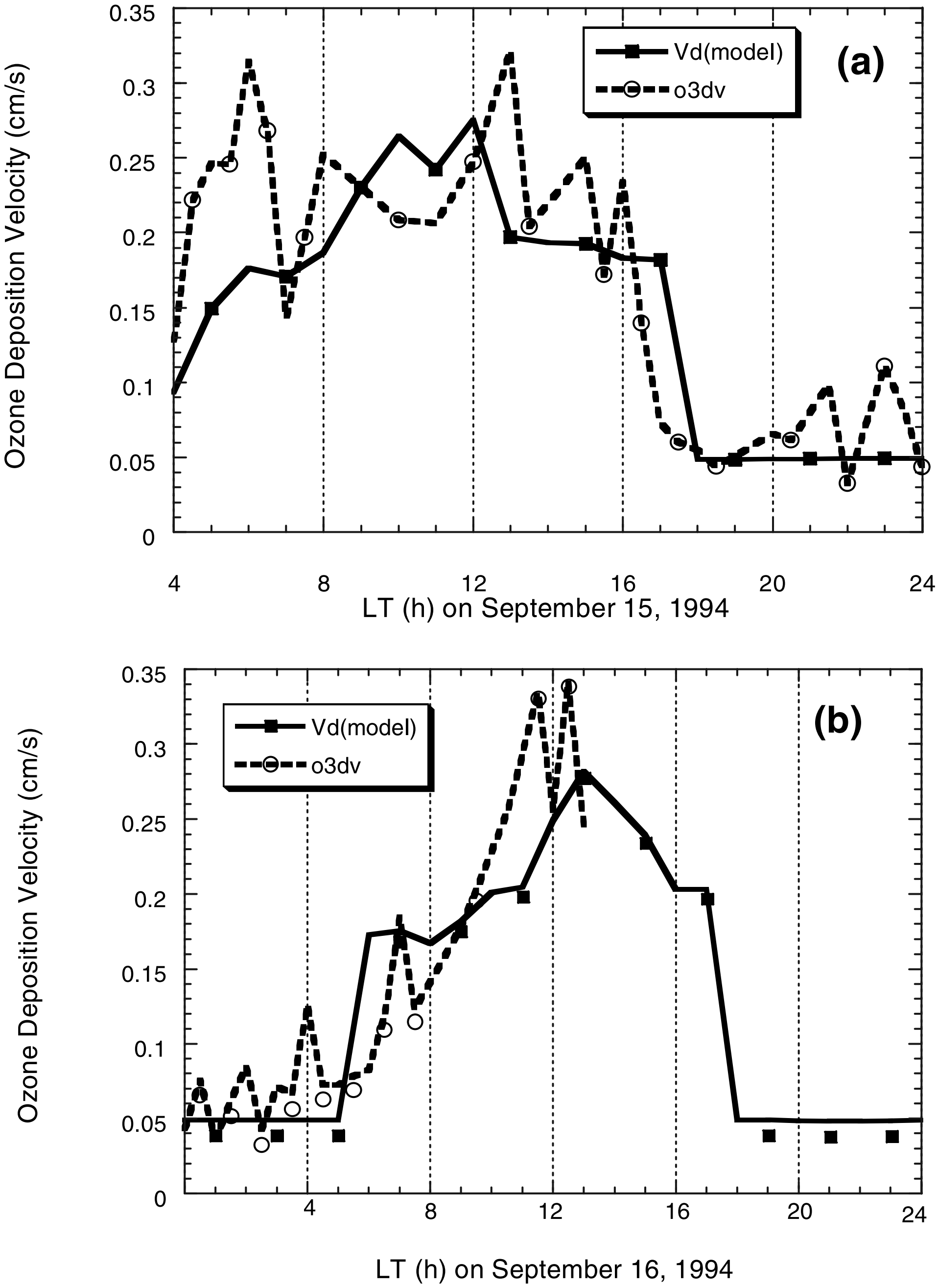

Figure 6. Observed (o3dv) and modeled ozone deposition velocity (cm s^{-1}) over a corn field near Bondville, IL, for (a) 15 September, 1994, and (b) 16 September, 1994. For this period, the vegetation was drying and less dense, and soil moisture availability was relatively high. For 16 September, observations are available only until noon.

al., 1997; Cooter and Schwede, 2000) that were not measured (e.g., soil moisture and soil texture). The observed variability at shorter time scales (minutes to hours) is attributable to factors such as the effect of interactions between the plant and the atmosphere (e.g. Su *et al*., 1996), cloud cover and the swaying of the crop and other factors affecting the plant response, which the model does not capture in big – leaf scaling. However, in general, the results provide an encouraging validation of the photosynthesis-based scheme for developing realistic V_d estimates over natural surfaces.

5. Summary and Conclusions

In an effort to parameterize the surface-atmosphere exchange over vegetation canopies, we considered a new deposition modeling approach that accounts for explicit canopy interactions in the surface-atmosphere exchanges. This canopy model is based on carbon assimilation (photosynthesis) and gas exchange concepts and is dynamically coupled to a prognostic land surface process routine and an atmospheric boundary layer model. Thus, the deposition velocities are estimated through a dynamically coupled (two-way) soil-vegetation-atmosphere continuum.

We validated the physiologically intensive V_d scheme using case studies over a soybean field (C3 photosynthesis pathway) and a corn field (C4 photosynthesis pathway) for which ozone deposition velocity observations are available. For the two cases, the model-simulated deposition velocity values showed good agreement with the observations, both in terms of the short-term (hourly) and the seasonal changes in the surface-atmosphere exchanges. This study has demonstrated that the photosynthesis-based approach can be efficiently applied for developing deposition velocity estimates over natural landscapes.

The model can also be used as a tool for generating ‘what if’ scenarios, particularly to ascertain and respond to ecological perturbations such as drought or carbon dioxide buildup, as well as to the effects of interactions among multiple gases depositing/competing for the surface. An interesting point regarding the initial conditions is that, for the Jarvis-type surface resistance schemes, the biophysical descriptors such as minimum stomatal resistance are largely uncertain and vary for each crop or species (Niyogi and Raman, 1997), while the gas-exchange-based constants are better correlated as a function of photosynthesis pathway (Ball *et al*., 1987) and classified based on land use category following Sellers *et al*. (1996). Additionally, the results suggest that model performance is generally better with higher soil moisture availability. Thus, future improvements in the model could include a more detailed representation of the effects of soil moisture on photosynthesis and gas deposition, and allowing the use of radiative components through multilayer vegetation in place of the big-leaf approach.

Acknowledgements

We sincerely thank Dr. Peter Finkelstein of the Air Resources Laboratory of the National Oceanic and Atmospheric Administration (NOAA/ERL/ARL) for providing the observations for ozone deposition velocity and surface meteorology from the field experiments used in this study. We also acknowledge Dr. Finkelstein as well as Dr. Bart Brasher and Dr. Ellen Cooter, both of NOAA/ERL/ARL, for several fruitful discussions on issues concerning surface-atmosphere exchanges. Parts of this study benefited through research funding from NOAA to the State Climate Office of North Carolina; and a NSF – Geoscience Education AFGE grant. however it has not been subjected to the agency's review process and no official endorsement should be inferred. The State Climate Office of North Carolina is a public service center at North Carolina State University for studying climate-environment interactions; it is funded in part by the College of Physical and Mathematical Science and the College of Agriculture and Life Science through the N.C. Agriculture Research Service. Numerical simulations were performed using computational resources provided by the North Carolina Supercomputing Center and are gratefully acknowledged. The NGM data were obtained from NOAA's READY server (www.arl.noaa.gov/READY).

Appendix

A-1. Photosynthesis/Plant model

The following discussion is based on the gas-exchange/photosynthesis based evapotranspiration model (GEM) described in Niyogi *et al.* (1999a, b, 2000). The vegetation module is based on the Ball-Woodrow-Berry stomatal model (Ball *et al.*, 1987; Niyogi and Raman, 1997) and the Collatz *et al.* (1991, 1992) photosynthesis scheme. The stomatal conductance (g_s) (inverse of resistance) is estimated as

$$g_s = m \frac{A_n rh_s}{C_s} + b \,, \tag{A-1}$$

where A_n is the net carbon assimilation (photosynthesis) rate, rh_s is the relative humidity, and C_s is the CO_2 concentration at the leaf surface. The terms m and b are constants based on gas-exchange considerations (Ball *et al.*, 1987) as a function of C3 or C4 vegetation and land use (Sellers *et al.*, 1996). In GEM, the physiological variables such as A_n, C_s, and rh_s at the leaf surface are estimated using evapotranspiration/photosynthesis relationships at the leaf scale.

Photosynthesis or carbon assimilation is taken as the residue of gross carbon assimilation (A_g) and loss due to respiration (R_d). Following Collatz *et al.* (1991, 1992),

$$A_g = \min \{W_c \text{ (rubisco-limited } A_g\text{)},$$

$$W_e \text{ (radiation-limited } A_g\text{)}, W_s \text{ (CO}_2\text{-limited } A_g\text{)}\} \ . \tag{A-2}$$

The carbon assimilation limiting rates are estimated as a function of photosynthesis pathway. For C3 vegetation,

$$W_c = V_m \left\{ \frac{C_i - \Gamma}{C_i + K_c(1 + O_2/K_o)} \right\} \tag{A-3a}$$

$$W_s = 0.5V_m \tag{A-3b}$$

$$W_e = PAR\varepsilon(1 - \omega_\pi)\cdot[(C_i - \Gamma)/(C_i + 2\Gamma)] \tag{A-3c}$$

while for C4 vegetation,

$$W_c = V_m \tag{A-4a}$$

$$W_e = PAR\varepsilon(1 - \omega_\pi) \tag{A-4b}$$

$$W_s = \frac{20000V_m C_i}{P} \tag{A-4c}$$

In the above, V_m is the maximum catalytic Rubisco capacity for the leaf; C_i is the carbon dioxide concentration in the leaf intercellular spaces; Γ is the CO_2 compensation point (Collatz *et al.*, 1992); O_2 is oxygen availability for the leaf; K_c and K_o are the Michaelis-Menten constant and the oxygen inhibition constant, respectively; *PAR* is the component of the total radiation available for photosynthetic activities; ε is the efficiency for carbon dioxide uptake; ω_π is the leaf-scattering coefficient for *PAR* (Sellers *et al.*, 1996); and P is the atmospheric pressure.

In the above, C_i is obtained through an iterative solution that includes net assimilation (A_n) and stomatal conductance (g_s).

The respiration loss R_d is estimated following Calvet *et al.* (1998) as,

$$R_d = 0.11A_m \tag{A-5}$$

where A_m is the maximum assimilation rate (Schulze *et al.*, 1994) which is limited by mesophyllic conductance (g_m) as,

$$A_m = A_{m,\max} \left\{ \frac{1 - \exp[-g_m(C_i - \Gamma)]}{A_{m,\max}} \right\} \ . \tag{A-6}$$

The mesophyllic conductance is related to the reactivity of the depositing gas (Wesley, 1989), and it also provides a link between available soil moisture and evapotranspiration, and effectively their control on deposition. Thus g_m is parameterized as (Calvet *et al.*, 1998),

$$g_m = g_{m,\max} 2^{Q_t} \frac{1 + \exp(0.3(T_c - S_2))}{1 + \exp(0.3(S_1 - T_c))} \cdot \frac{(w_2 - w_{wilt})}{(w_{sat} - w_{wilt})} \ , \tag{A-7}$$

where $g_{m,\max}$ is typically 17.5×10^{-3} ms^{-1}, Q_t is the 'Q-10 term': temperature – modulation of the biophysical characteristics, T_c is the surface temperature, S_1 and S_2 are land-use-based coefficients as described in Sellers *et al.* (1996), and w_2, w_{wilt}, and w_{sat} are the deep (∼root-level) soil moisture and the wilting and saturation capacity of the soil, respectively. For the CO_2 concentration at the leaf surface (C_s) we use

$$C_s = C_a - (A_n \cdot R_b) \;, \tag{A-8}$$

where, C_a is the ambient CO_2 concentration. For closure, using an approach similar to that of Collatz *et al.* (1991), C_i is estimated as

$$C_i = C_s - (\eta \cdot A_n \cdot P \cdot R_b) \;. \tag{A-9}$$

Typical values of η are 1.6 for carbon dioxide, nitrous acid, ozone, and nitrogen dioxide; 1.9 for sulfur dioxide and nitric acid; 1.3 for nitrous oxide; and 1.0 for ammonia (Wesely, 1989).

A-2. Atmospheric and Soil Model

The atmospheric and soil models are similar to those described in Alapaty *et al.* (1997). To achieve a fully coupled two-way interaction between the surface and the atmosphere, the GEM-based physiological resistance module is linked to a detailed PBL and land surface process (LSP) model (Noilhan and Planton, 1989; Alapaty *et al.*, 1997). At the core of the model, five equations are solved prognostically for topsoil (0.1 m) and deep-soil (1 m) temperature (T_{g1}, T_{g2}) and moisture (W_{g1}, W_{g2}), and rainfall interception (W_r):

$$\frac{\partial T_{g1}}{\partial t} = C_T(R_n - S_{hf} - L_{hf}) - \frac{2\pi}{\tau}\left(T_{g1} - T_{g2}\right) \tag{A-10}$$

$$\frac{\partial T_{g2}}{\partial t} = \frac{(T_{g1} - T_{g2})}{\tau} \tag{A-11}$$

$$\frac{\partial W_{g1}}{\partial t} = \frac{C_1}{\rho_w d_1}\left(P_g E_g\right) - \frac{C_2}{\tau}\left(W_{g1} - W_{geq}\right) \tag{A-12}$$

$$\frac{\partial W_{g2}}{\partial t} = \frac{(P_g - E_g - E_{tr})}{\rho_w d_2} \tag{A-13}$$

$$\frac{\partial W_r}{\partial t} = (V_c P_r) - E_r \;. \tag{A-14}$$

In the above, C_T is the thermal transfer coefficient, while C_1 and C_2 are soil moisture coefficients (Noilhan and Planton, 1989); R_n, S_{hf} and L_{hf} are net radiation, sensible heat, and latent heat fluxes at the surface, π is total seconds in a day, ρ_w is the density of liquid water, d_1 and d_2 are the thicknesses of the two soil layers, P_g is the flux of liquid water reaching the soil surface, E_g is the evaporation at the soil surface, W_{geq} is the topsoil moisture when gravity balances the capillary forces, E_{tr} is the transpiration rate, V_c is the fractional vegetation cover, P_r is the precipitation rate at the top of the vegetation, and E_r is the evaporation rate from the wet parts of the canopy. Total evaporation from the surface is taken as the sum of E_g, E_{tr}, and E_r, and is provided as a surface boundary condition to the atmospheric model. In the atmospheric model, net radiation at the surface is the sum of incoming solar radiation (a function of solar zenith angle, surface albedo, and atmospheric turbidity), atmospheric longwave back-scattering radiation, and outgoing longwave surface radiation (Anthes *et al*., 1987; Pleim and Xiu, 1995). Upward and downward longwave radiation are calculated as functions of soil emissivity, ground temperature, atmospheric longwave emissivity, and atmospheric temperatures. Additionally, the PBL model uses surface layer similarity relationships with a turbulent kinetic energy (TKE) approach for the mixed-layer parameterization. More details regarding these submodels can be found in Alapaty *et al*. (1997).

References

Alapaty, K., Pleim, J. E., Raman, S., Niyogi, D. S. and Byun, D.: 1997, 'Simulation of atmospheric boundary layer processes using local- and nonlocal-closure schemes', *J. Appl. Meteor.* **36**, 214–233.

Anthes, R., Hsie, E. and Kuo, Y.: 1987, 'Description of the Penn State/NCAR Mesoscale Model Version 4 (MM4)', *NCAR Tech. Note NCAR/TN-282 + STR*, 66 pp.

Arya, S. P. S.: 1988, *Introduction to Micrometeorology*, Academic Press, San Diego, 308 pp.

Avissar, R., Avissar, P., Mehrer, Y. and Bravdo, B.: 1985, 'A model to simulate response of plant stomata to environmental conditions', *Agric. For. Meteorol.* **34**, 21–29.

Baldocchi, D., Hicks, B. B. and Camara, P.: 1988, 'A canopy stomatal resistance model for gaseous deposition to vegetated surfaces', *Atmos. Environ.* **21**, 91–101.

Ball, J., Woodrow, I. and Berry, J.: 1987, 'A Model Predicting Stomatal Conductance and Its Contribution to the Control of Photosynthesis under Different Environmental Conditions', in *Progress in Photosynthesis Research*, Vol. IV, Martinus Nijhoff Pub., Dordrecht, pp. 221–224.

Businger, J., Wyngaard, J., Izum, Y. and Bradley, E.: 1971, 'Flux-profile relationship in the atmospheric surface layer', *J. Atmos. Sci.* **28**, 181–189.

Calvet, J.-C., Noilhan, J., Roujean, J., Bessemoulin, P., Cabelguenne, M., Olioso, A. and Wigneron, J.: 1998, 'An interactive vegetation SVAT model tested against data from six contrasting sites', *Agric.-Forest. Meteor.* **92**, 73–95.

Calvet, J.-C., Bessemoulin, P., Noilhan, J., Berne, C., Braud, I., Courault, D., Fritz., N., Gonzalez-Sosa, E., Goutorbe, J., Haverkamp, R., Jaubert, G., Kergoat, L., Lachaud, G., Laurent, J., Mordelet, P., Olioso, A., Peris, P., Roujean, J., Thony, J., Tosca, C., Vauclin, M. and Vignes, D.: 1999, 'MUREX: A land–surface field experiment to study the annual cycle of the energy and water budgets', *Ann. Geophys.* **17**, 838–854.

Chang, J., Brost, R., Isaksen, I., Madronich, P., Middleton, P., Stockwell, W. and Walcek, C.: 1987, 'A three-dimensional eulerian acid deposition model: Physical concepts and formulation', *J. Geophys. Res.* **92**, 14681–14700.

Collatz, G. J., Ball, J., Grivet, C. and Berry, J.: 1991, 'Physiological and environmental regulation of stomatal conductance, photosynthesis and transpiration: A model that includes a laminar boundary layer', *Agri. For. Meteor.* **54**, 107–136.

Collatz, G. J., Ribas-Carbo, M. and Berry, J.: 1992, 'Coupled photosynthesis-stomatal conductance model for leaves of C4 plants', *Aust. J. Plant Physiol.* **19**, 519–538.

Cooter, E. J. and Schwede D.: 2000, 'Sensitivity of the national oceanic and atmospheric administration multiplayer model to instrument error and parameterization uncertainty', *J. Geophys. Res.* **105**, 6695–6704.

Davenport, A., Grimmond, S., Oke, T. and Wieringa, J.: 2000, 'Estimating the Roughness of Cities and Sheltered Country', *12th AMS Conference on Applied Climatology*, Asheville, NC, 8–11 May 2000, Amer. Meteor. Soc., Boston, MA, pp. 96–99.

Draxler, R. R. and Hess, G.: 1997, 'Description of the HySplit-4 Modeling System', NOAA Tech. Mem. ERL/ARL-224 (Available from http://www.arl.noaa.gov/READY).

Erisman, J., Beier, C., Draaijers, G. and Lindberg, S.: 1994, 'Review of deposition monitoring methods', *Tellus* **46**, 79–93.

Farquhar, G. D., von Caemmerer, S. and Berry, J.: 1980, 'A biochemical model of photosynthetic CO_2 assimilation in leaves of C3 species', *Planta* **149**, 78–90.

Finkelstein, P., Ellestad, T., Clarke, J., Meyers, T., Schwede, D., Hebert, E. and Neal, J.: 2000, 'Ozone and sulfur dioxide dry deposition to forests: Observations and model evaluation', *J. Geophys. Res.* **105**, 15365–15378.

Fowler, D., Flechard, C., Sutton, M. and Storeton-West, R.: 1998, 'Long-term measurements of the land-atmosphere exchange of ammonia over moorland', *Atmos. Eviron.* **32**, 453–459.

Garland, J.: 1977, 'The dry deposition of sulphur dioxide to land and water surfaces', *Proc. Roy. Soc. Lond.* **534A**, 245–268.

Giorio, P., Sorrentino, G. and d'Andria, R.: 1999, 'Stomatal behaviour, leaf wetness status and photosynthetic response in field-grown olive trees under water deficit', *Environ. Expt. Bot.* **42**, 95–104.

Hampp, R.: 1992, 'Comparative evaluation of the effects of gaseous pollutants, acidic deposition and mineral deficiencies on the carbohydrate metabolism of trees', *Ag. Ecosys. Econ.* **42**, 333–351.

Hicks, B. B., and Matt, D.: 1988, 'Combining biology, chemistry, and meteorology in modeling and measuring dry deposition', *J. Atmos. Chem.* **6**, 117–131.

Hoke, J., Phillips, N., DiMego, G., Tuccillo, J. and Sela, J.: 1989, 'The regional analysis and forecast system of the National Meteorological Center', *Weather and Forecasting* **4**, 323–334.

Jarvis, P.: 1976, 'The interpretation of leaf water potential and stomatal conductance found in canopies in the field', *Phil. Trans. R. Soc. Lond* **B 273**, 593–610.

Kramm, G., Beier, N., Foken, T., Muller, H., Schroder, P. and Seiler, W.: 1996, 'A SVAT for NO, NO_2, and O_3-model description and test results', *Meteor. Atmos. Physics* **61**, 89–106.

Makela, A., Berninger, F. and Hari, P.: 1996, 'Optimal control of gas exchange during drought: Theoretical analysis', *Ann. Bot.* **77**, 461–467.

Meyers, T., Finkelstein, P., Clarke, J., Ellestad, T. and Sims, P.: 1998, 'A multilayer model for inferring dry deposition using standard meteorological measurements', *J. Geophys. Res.* **103**, 22645–22661.

Mellor, R. and Yamada, T.: 1974, 'A hierarchy of turbulence closure models for planetary boundary layers', *J. Atmos. Sci.* **31**, 1791–1806.

Musselman, R. and Minnick, T.: 2000, 'Nocturnal stomatal conductance and ambient air quality standards for ozone', *Atmos. Environ.* **34**, 719–733.

NCDENR: 1999, *Air Quality Research Needs and Programs in North Carolina*, Division of Air Quality, North Carolina Department of Environment and Natural Resources, Raleigh, NC, 57 pp.

NRC: 2000, *Clean Coastal Waters: Understanding and Reducing the Effects of Nutrient Pollution*, National Research Council, National Academy Press, Washington, DC, 405 pp.

Nemitz, E., Sutton, M., Gut, A., Jose, R., Husted, S. and Schjoerring, J.: 2000, 'Sources and sinks of ammonia within an oilseed rape canopy', *Agric. Forest Meteor.* **105**, 385–404.

Nikolov, N., Massman, W. and Schoettle, A.: 1995, 'Coupling biochemical and biosphysical processes at the leaf level: An equilibrium photosynthesis model for leaves of C3 plants', *Ecol. Mod.* **80**, 205–235.

Niyogi, D. S.: 2000, 'Biosphere–Atmosphere Interactions Coupled with Carbon Dioxide and Soil Moisture Changes', *Ph.D. Dissertation*, Dept. of Marine, Earth, and Atmos. Sci., North Carolina State University, Raleigh, NC 27695, 509 p.

Niyogi, D. S. and Raman, S.: 1997, 'Comparison of four different stomatal resistance schemes using FIFE observations', *J. Appl. Meteor.* **36**, 903–917.

Niyogi, D. S. and Raman, S.: 2000, 'Numerical Modeling of Gas Deposition and Bi-directional Surface-Atmosphere Exchanges in Mesoscale Air Pollution Systems', in Z. Boybeyi (ed.), *Mesoscale Dispersion Modeling*, Computational Mechanics Publications, Southampton, U.K., 424 p.

Niyogi, D. S., Raman, S. and Alapaty, K.: 1998, 'Comparison of four different stomatal resistance schemes using FIFE observations, Part 2: Analysis of terrestrial biospheric–atmospheric interactions', *J. Appl. Meteor.* **37**, 1301–1320.

Niyogi, D. S., Alapaty, K. and Raman, S.: 1999b, 'An Advanced Carbon Assimilation Surface Evapotranspiration Scheme for Mesoscale Models', *MM5 Workshop on Land Surface Modeling and its Application to Mesoscale Models*, 24–25 June 1999, Boulder, CO.

Niyogi, D. S., Alapaty, K. and Raman, S.: 1999c, 'Developing Multi-media Couplings to Link Ambient Meteorological Information with Depositing Surface Environment', *Workshop on Atmospheric Nitrogen Compounds: Emissions Transport, Transformation, Deposition, and Assessment*, 7–9 June 1999, Chapel Hill, NC, pp. 355–371.

Niyogi, D. S., Raman, S. and Alapaty, K.: 1999d, 'Uncertainty in specification of surface characteristics, Part 2: Hierarchy of interaction explicit statistical analysis', *Bound.-Layer Meteor.* **91**, 341–366.

Niyogi, D. S., Raman, S., Alapaty, K. and Hopkins, T.: 1999a, 'An Integrated Dynamic, Physiochemical Approach to Assessing the Transport and Deposition of Chemical Species in Eastern North Carolina', *Workshop on Atmospheric Nitrogen Compounds: Emissions Transport, Transformation, Deposition, and Assessment*, 7–9 June 1999, Chapel Hill, NC., pp. 383–396.

Niyogi, D. S., Alapaty, K. and Raman, S.: 2000, 'A gas exchange based surface evapotranspiration model (GEM) for mesoscale applications', *Agric. For. Meteorol.* (submitted).

Noilhan, J. and Planton, S.: 1989, 'A simple parameterization of land surface processes for meteorological models', *Mon. Wea. Rev.* **117**, 536–549.

Padro, J.: 1994, 'Observed Characteristics of the dry deposition velocity of O_3 and SO_2 above a wet deciduous forest', *Sc. Tot. Environ.* **146/147**, 395–400.

Pleim, J. and Xiu, A.: 1995, 'Development and testing of a surface flux planetary boundary layer model with explicit soil moisture parameterization for applications in mesoscale models', *J. Appl. Meteor.* **34**, 16–32.

Rondon, A. and Grana, L.: 1994, 'Studies on the dry deposition of NO_2 to coniferous species at low NO_2 concentrations', *Tellus* **46B**, 339–352.

Schulze, E., Kelliher, F., Korner, C., Lloyd, J. and Leuning, R.: 1994, 'Relationships among maximum stomatal conductance, ecosystem surface conductance, carbon assimilation rate, and plant nitrogen nutrition: A global ecology scaling exercise', *Annu. Rev. Ecol. Syst.* **25**, 629–660.

Sellers, P., Hall, F., Asrar, G., Strebel, D. and Murphy, R.: 1988, 'The first ISLSCP experiment (FIFE)', *Bull. Amer. Meteor. Soc.* **69**, 22–27.

Sellers, P., Randall, D., Collatz, J., Berry, J., Field, C., Dazlich, D., Zhang, C., Collelo, G. and Bounous, A.: 1996, 'A revised land surface parameterization (SiB2) for atmospheric GCMs: Model formulation', *J. Clim.* **9**, 676–705.

Shaw, R. and Periera, A.: 1982, 'Aerodynamic roughness of plant canopy: A numerical experiment', *Agric. Meteor.* **26**, 51–65.

Su, H., Paw, U. K. and Shaw, R.: 1996, 'Development of a coupled leaf and canopy model for the simulation of plant–atmosphere interaction', *J. Appl. Meteorol.* **35**, 734–748.

Sutton, M., Burkhardt, J., Guerin, D., Nemitz, E. and Fowler, D.: 1998, 'Development of resistance models to describe measurements of bi-directional ammonia surface–atmosphere exchange', *Atmos. Environ.* **32**, 473–480.

Valigura, R., Alexander, R., Brock, D., Castro, M., Meyers, T., Paerl, H., Stacey, P. and Stanley, D. (eds.): 2000, *An Assessment of Nitrogen Inputs to Coastal Areas with an Atmospheric Perspective*, AGU Coastal Estuaries Series, American Geophysical Union, Washington DC, 252 pp.

Walmsley, P. and Wesely, M.: 1996, 'Modification of coded parameterizations of surface resistances to gaseous dry deposition', *Atmos. Environ.* **30**, 1181–1196.

Wesely, M.: 1989, 'Parameterization of surface resistance to gaseous dry deposition in regional scale numerical models', *Atmos. Environ.* **23**, 1293–1304.

Wesely, M. and Hicks, B.: 2000, 'A review of the current status of knowledge on dry deposition', *Atmos. Environ.* **34**, 2261–2282.

Wieringa, J.: 1993, 'Representative roughness parameters for homogeneous terrains', *Bound.-Layer Meteor.* **63**, 323–363.